VELOCITY, MASS AND TEMPERATURE ANALYSIS OF FREE CONVECTIVE MHD SECOND GRADE FLUID FLOW PAST AN EXPONENTIALLY ACCELERATED VERTICAL PLATE IN THE PRESENCE OF THERMO-DIFFUSION AND HEAT GENERATION / ABSORPTION THROUGH POROUS MEDIUM

Rakesh R. Darji

Assistant Professor,
Applied Science & Humanities Department,
SardarVallabhbhai Patel Institute of Technology, Vasad, Gujarat, India

Abstract : ***This paper is concerned with the study of flow, heat and mass transfer characteristics on the free convection MHD flow of second grade fluid past an exponentially accelerated vertical plate. It is assumed that the bounding plate has a ramped temperature and isothermal temperature in a porous medium. Analytic solution of momentum, energy and concentration equations are obtained in closed form by Laplace transform technique. From velocity, temperature and concentration fields, the exact expression of skin friction, Nusselt number and Sherwood number are derived. The results obtained show the impact of Prandtl number Pr, Grashof number Gr, Gm, Schmidt number Sc, magnetic parameter M, Soret number Sr, heat generation / absorption parameter H and time t on velocity, heat and mass transfer and clarified with the help of graphical illustrations.***

Keywords: Magneto hydrodynamics; Second grade fluid, isothermal temperature; Ramped temperature; Skin friction; Nusselt number; Sherwood number.

I. Introduction

The non-Newtonian fluids are considered as more appropriate models of fluids in industrial and technological applications than Newtonian fluids. Non-Newtonian fluid flow analysis is much more complicated and subtle in comparison with Newtonian fluids. The governing equations are very complex and the solutions of the resulting equations are more difficult to obtain. Due to the complexity of fluids, several models of non-Newtonian fluids have been proposed in the literature. Second grade fluid is one of the non-Newtonian fluids. M. Sheikholeslami [1-2] has introduced influence of EFD viscosity on nanofluid forced than M. Sheikholeslami and M. M. Bhatti [3] have done research work on nanofluid heat transfer enhancement by means of EHD.

S.A. Shehzad and M. Sheikholeslami [4] studied thermal radiation of Lorentz forces considering viscosity. T. Hayat et al. [5] studied numerical simulation of nanofluid forced convection heat transfer. M. Shamlooei and M. Sheikholeslami [6] discussed natural convection in presence of thermal radiation. M. Sheikholeslami [7] and T. Hayat et al. [8] obtained numerical solution of MHD nanofluid free convective heat transfer. On the other hand, flow in porous media has practical applications in heat removal from debris, storage of food stuffs, paper production, nuclear fuel, oil exploration, underground disposal of radioactive waste material etc. Some of related research studies are due to Kataria and Mittal [9-10]. M.M. Rashidi et al. [11-16] discussed unsteady MHD free convective flow with numerical technique. M Hatami et al. [17-21] studied hydrodynamic heat transfer. D D Ganji et al. [22-26] studied micropolar fluid flow and heat transfer. Katariya and Patel [27-31] obtained analytic solution of MHD fluid flow with ramped wall temperature through porous medium. H R Seyf et al. [32] discussed heat transfer through a porous using two-equation energy model. S M Rassoulinejad-Mousavi and S Abbasbandy [33] did analysis in a circular tube using Homotopy analysis method. S M Rassoulinejad-Mousavi et al. [34-37] discussed fluid flow in moving wall. Due to increasing significant, Application of unsteady second grade MHD flow with heat and mass transfer is important in engineering and technology. Many researchers like, Cortell [38], Hayat et al. [39-42]. Bataineh et al. [43] obtained the solution using bernstein method for the MHD flow and heat transfer of a second grade fluid in a channel with porous wall.

In present investigation, we have studied Analytic expression of MHD second grade fluid flow past an exponentially accelerated in the presence of thermal radiation and concentration with ramped wall temperature and ramped surface concentration through porous medium is obtained using Laplace transform technique.

Nomenclature:

B_0 Uniform magnetic field	k' Permeability of porous medium
u' Fluid velocity	$q_r{}'$ Radiative heat flux
t' Time	u Dimensionless fluid velocity
T' Fluid temperature	θ Dimensionless fluid temperature

C' Species concentration
C_p Specific heat at constant pressure
D_M Mass diffusion coefficient
k Permeability parameter
Pr Prandtl number
Sc Schmidt number
H Heat generation Parameter
C Dimensionless concentration
Gm Mass Grashof number
Gr Thermal Grashof number
R Thermal Radiation
M Magnetic parameter
t Dimensionless time
Sr Soret Number

Greek symbols:
φ Porosity of the porous medium
ν Kinematic viscosity coefficient
β'_T Volumetric coefficient of thermal expansion
β'_c Volumetric coefficient of concentration expansion
α_1 One of the material modules of second grade fluids.
ρ Fluid density
g Acceleration due to gravity
σ Electrical conductivity
k_1 -Thermal conductivity
α Second grade parameter

II. MATHEMATICAL FORMULATION OF THE PROBLEM:

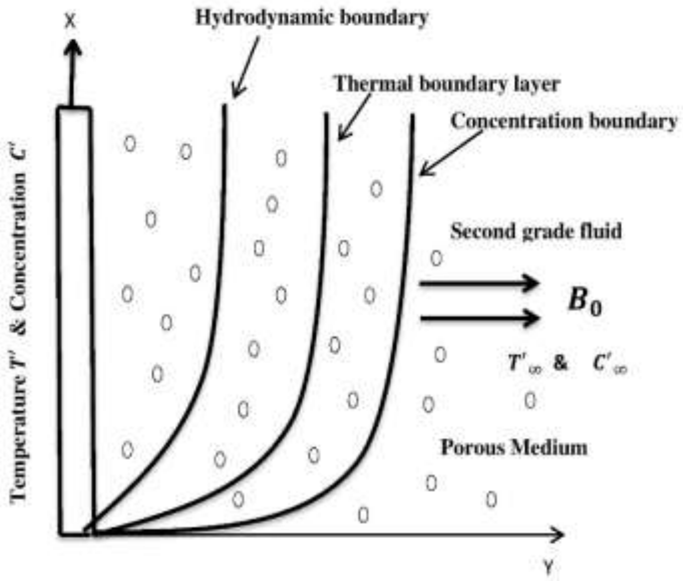

$$Where,\ T' = \begin{cases} T'_\infty + (T'_w - T'_\infty)\,{t'}/{t_0} & if\ 0 < t' < t_0 \\ T'_w & if\ \ t' \geq t_0 \end{cases},\quad C' = \begin{cases} C'_\infty + (C'_w - C'_\infty)\,{t'}/{t_0} & if\ 0 < t' < t_0 \\ C'_w & if\ \ t' \geq t_0 \end{cases};\ y' = 0$$

Figure 1: Physical sketch of the problem

In Figure 1, Coordinate system is considered $x' - axis$ is taken along the wall in the upward direction and $y' - axis$ is taken normal to it. In $y' - axis$ direction transverse magnetic field of strength B_0 is applied uniformly.Initially, at time$t' \leq 0$, both the fluid and the plate are constant temperature T'_∞ and concentration near the plate is assumed to be C'_∞respectively. At the time$t' > 0$, temperature& concentration of the wall is raised or lowered to $T'_\infty + (T'_w + T'_\infty)\,{t'}/{t_0}$ &$C'_\infty + (C'_w - C'_\infty)\,{t'}/{t_0}$ when $t' \leq t_0$ and T'_w&$C'_w$when $t' > t_0$ respectively which is there after maintained constantT'_w&C'_w. It is assumed that the effects of viscous dissipation in energy equation, induce magnetic and electrical field are negligible also assume that flow is incompressible, laminar, uni-direction, one dimensional. Under above assumptions and taking into account the Boussinesq's approximation, governing equations are given below:

$$\frac{\partial u'}{\partial t'} = \left(\nu + \frac{\alpha_1}{\rho}\frac{\partial}{\partial t'}\right)\frac{\partial^2 u'}{\partial y'^2} + g\beta'_T(T' - T'_\infty) - \frac{\sigma B_0{}^2}{\rho}u' - \frac{\varphi}{k'}\left(\nu + \frac{\alpha_1}{\rho}\frac{\partial}{\partial t'}\right)u' + g\beta'_C(C' - C'_\infty) \tag{1}$$

$$\frac{\partial T'}{\partial t'} = \frac{k_1}{\rho c_p}\frac{\partial^2 T'}{\partial y'^2} + \frac{Q_0}{\rho c_p}(T' - T'_\infty) \tag{2}$$

$$\frac{\partial C'}{\partial t'} = D_M\frac{\partial^2 C'}{\partial y'^2} + D_T\frac{\partial^2 T'}{\partial y'^2} \tag{3}$$

Where following initial and boundary condition:

$$u' = 0,\quad T' = T'_\infty,\quad C' = C'_\infty;\ as\ \ y' \geq 0\ and\ \ t' \leq 0$$

$$u' = e^{at'}\ ,\ T' = \begin{cases} T'_\infty + (T'_w - T'_\infty)\,{t'}/{t_0} & if\ \ 0 < t' \leq t_0 \\ T'_w & if\ \ \ t' \geq t_0 \end{cases},$$

$$C' = \begin{cases} C'_\infty + (C'_w - C'_\infty)\,{t'}/{t_0} & if\ \ 0 < t' \leq t_0 \\ C'_w & if\ \ \ t' \geq t_0 \end{cases};\ \ as\ \ t' > 0\ and\ y' = 0$$

$$u' \to 0, T' \to T'_\infty,\ \ C' \to C'_\infty;\ as\ \ y' \to \infty\ and\ t' \geq 0 \tag{4}$$

Introducing the following dimensionless quantities:

$$y = \frac{y'}{\sqrt{\nu t_0}}, u = \sqrt{\frac{t_0}{\nu}}u', t = \frac{t'}{t_0}, \alpha = \frac{\alpha_1}{\rho\, \nu\, t_0}, Gr = \frac{t_0^{\,3/2}\, g\beta'_T(T'_w - T'_\infty)}{\sqrt{\nu}}, M^2 = \frac{\sigma B_0^2}{\rho}t_0^{\,2}, \frac{1}{k} = \frac{\nu t_0^{\,2}\,\varphi}{k'},$$

$$Gm = \frac{t_0^{\,3/2}\, g\beta'_C(C'_w - C'_\infty)}{\sqrt{\nu}}, \theta = \frac{(T' - T'_\infty)}{(T'_w - T'_\infty)}, C = \frac{(C' - C'_\infty)}{(C'_w - C'_\infty)}, P_r = \frac{\rho\nu C_p\, t_0}{k_1}, H = \frac{Q_0 \nu^2}{\rho c_p k\, U_0^2},$$

$$Sc = \frac{\nu t_0}{D_M}, Sr = \frac{D_T(T'_w - T'_\infty)}{\nu(C'_w - C'_\infty)}$$

$$c = 1 + \frac{\alpha}{k}, b = M^2 + \frac{1}{k}$$

In the equations (1-4) dropping out the " ′ "notation (for simplicity) we get

$$\frac{\partial^2 u}{\partial y^2} + \alpha\frac{\partial^3 u}{\partial y^2 \partial t} - c\frac{\partial u}{\partial t} - bu + Gr\theta + Gm\, C = 0 \qquad (5)$$

$$\frac{\partial \theta}{\partial t} = \frac{1}{Pr}\frac{\partial^2 \theta}{\partial y^2} + H\theta \qquad (6)$$

$$\frac{\partial C}{\partial t} = \frac{1}{Sc}\frac{\partial^2 C}{\partial y^2} + Sr\frac{\partial^2 \theta}{\partial y^2} \qquad (7)$$

With initial and boundary conditions

$$u = \theta = C = 0, \qquad y \geq 0, t = 0$$

$$u = e^{at}, \ \theta = \begin{cases} t, & 0 < t \leq 1 \\ 1 & t > 1 \end{cases} = tH(t) - (t-1)H(t-1),$$

$$C = \begin{cases} t, & 0 < t \leq 1 \\ 1 & t > 1 \end{cases} = tH(t) - (t-1)H(t-1), \quad y = 0, \quad t > 0$$

$$u \to 0, \theta \to 0, C \to 0 \quad as \ y \to \infty, t > 0 \qquad (8)$$

Where H (.) is Heaviside unit step function.

III. SOLUTION:

Taking Laplace transform of equations (5-7) with initial and boundary conditions (8)

$$\bar{\theta} = F_{15}(y,s)(1 - e^{-s}) \qquad (9)$$

$$\bar{C} = H_1(y,s)(1 - e^{-s}) + H_2(y,s)(1 - e^{-s}) \qquad (10)$$

$$\bar{u}(y,s) = F_1(y,s) + F_{10}(y,s)(1 - e^{-s}) + F_{11}(y,s)(1 - e^{-s}) + F_{12}(y,s)(1 - e^{-s}) \qquad (11)$$

Where

$$F_1(y,s) = \frac{1}{s-a}e^{-y\sqrt{\frac{cs+b}{\alpha s+1}}} \qquad (12)$$

$$F_2(y,s) = \frac{1}{s}e^{-y\sqrt{\frac{cs+b}{\alpha s+1}}} \qquad (13)$$

$$F_3(y,s) = \frac{1}{s}e^{-y\sqrt{\Pr(s-H)}} \qquad (14)$$

$$F_4(y,s) = \frac{1}{s}e^{-y\sqrt{\mathrm{Sc}\, s}} \qquad (15)$$

$$F_5(y,s) = F_2(y,s) - F_3(y,s) \qquad (16)$$

$$F_6(y,s) = F_2(y,s) - F_4(y,s) \qquad (17)$$

$$F_7(y,s) = \frac{a_{20}}{s} + \frac{a_{21}}{s-b_4} + \frac{a_{22}}{s-b_5} \qquad (18)$$

$$F_8(y,s) = \frac{a_{23}}{s} + \frac{a_{24}}{s-b_9} + \frac{a_{25}}{s-b_{10}} + \frac{a_{26}}{s-a_5} \qquad (19)$$

$$F_9(y,s) = \frac{a_{27}}{s} + \frac{a_{28}}{s-b_4} + \frac{a_{29}}{s-b_5} + \frac{a_{30}}{s-a_{16}} \qquad (20)$$

$$F_{10}(y,s) = F_5(y,s)F_7(y,s) \qquad (21)$$

$$F_{11}(y,s) = F_6(y,s)F_8(y,s) \qquad (22)$$

$$F_{12}(y,s) = F_5(y,s)F_9(y,s) \qquad (23)$$

$$F_{13}(y,s) = \frac{1}{s^2}e^{-y\sqrt{\mathrm{Sc}\, s}} \qquad (24)$$

$$F_{14}(y,s) = \frac{1}{s-a_5}e^{-y\sqrt{\mathrm{Sc}\, s}} \qquad (25)$$

$$F_{15}(y,s) = \frac{1}{s^2}e^{-y\sqrt{\Pr(s-H)}} \qquad (26)$$

$$F_{16}(y,s) = \frac{1}{s-a_{16}}e^{-y\sqrt{\Pr(s-H)}} \qquad (27)$$

$$H_1(y,s) = a_{10}F_4(y,s) + a_8F_{13}(y,s) + a_9F_{14}(y,s) \qquad (28)$$

$$H_2(y,s) = a_{19}F_3(y,s) + a_{17}F_{15}(y,s) + a_{18}F_{16}(y,s) \qquad (29)$$

Taking Inverse Laplace transform of equation (9) to (11), we get

$$\theta(y,t) = f_{15}(y,t) - f_{15}(y,t-1)H(t-1) \qquad (30)$$

$$C(y,t) = h_1(y,t) - h_1(y,t-1)H(t-1) + h_2(y,t) - h_2(y,t-1)H(t-1) \qquad (31)$$

$$u = f_1(y,t) + f_{10}(y,t) - f_{10}(y,t-1)H(t-1) + f_{11}(y,t) - f_{11}(y,t-1)H(t-1) + f_{12}(y,t) - f_{12}(y,t-1)H(t-1) \qquad (32)$$

Where

$$f_1(y,t) = L^{-1}\left[\frac{1}{s-a}e^{-y\sqrt{\frac{cs+b}{\alpha s+1}}}\right] \qquad (33)$$

$$f_2(y,t) = \frac{c}{\alpha}e^{-t/\alpha}\int_0^\infty erfc\left(\frac{y}{2\sqrt{z}}\right)e^{-c/\alpha\, z}I_0\left(\frac{2}{\alpha}\sqrt{(c-\alpha b)zt}\right)dz + \frac{b}{\alpha}\int_0^\infty\int_0^t erfc\left(\frac{y}{2\sqrt{z}}\right)e^{-\frac{cz+s}{\alpha}}I_0\left(\frac{2}{\alpha}\sqrt{(c-\alpha b)zs}\right)ds\, dz \qquad (34)$$

Where

I_0- Bessel function and $erfc\ (g)$- complementary error function.

$$f_3(y,t)=\frac{1}{2}\left[e^{-y\sqrt{-HPr}}\,erfc\left(\frac{y}{2\sqrt{t/Pr}}-\sqrt{-Ht}\right)+e^{y\sqrt{-HPr}}\,erfc\left(\frac{y}{2\sqrt{t/Pr}}+\sqrt{-Ht}\right)\right] \quad (35)$$

$$f_4(y,t)=erfc\left(\frac{y\sqrt{S_c}}{2\sqrt{t}}\right) \quad (36)$$

$$f_5(y,t)=f_2(y,t)-f_3(y,t) \quad (37)$$

$$f_6(y,t)=f_2(y,t)-f_4(y,t) \quad (38)$$

$$f_7(y,t)=a_{20}+a_{21}e^{b_4t}+a_{22}e^{b_5t} \quad (39)$$

$$f_8(y,t)=a_{23}+a_{24}e^{b_9t}+a_{25}e^{b_{10}t}+a_{26}e^{a_5t} \quad (40)$$

$$f_9(y,t)=a_{27}+a_{28}e^{b_4t}+a_{29}e^{b_5t}+a_{30}e^{a_{16}t} \quad (41)$$

$$f_{10}(y,t)=f_5(y,t)*f_7(y,t) \quad (42)$$

$$f_{11}(y,t)=f_6(y,t)*f_8(y,t) \quad (43)$$

$$f_{12}(y,t)=f_5(y,t)*f_9(y,t) \quad (44)$$

$$f_{13}(y,t)=\left(\frac{y^2S_c}{2}+t\right)erfc\left(\frac{y\sqrt{S_c}}{2\sqrt{t}}\right)-\frac{y\sqrt{S_ct}}{2\sqrt{\pi}}e^{-\frac{y^2S_c}{4t}} \quad (45)$$

$$f_{14}(y,t)=\frac{e^{a_8t}}{2}\left[e^{-y\sqrt{S_ca_5}}\,erfc\left(\frac{y\sqrt{S_c}}{2\sqrt{t}}-\sqrt{a_5t}\right)+e^{y\sqrt{S_ca_5}}\,erfc\left(\frac{y\sqrt{S_c}}{2\sqrt{t}}+\sqrt{a_5t}\right)\right] \quad (46)$$

$$f_{15}(y,t)=\frac{1}{2}\left[\left(t-\frac{y}{2\sqrt{-H/Pr}}\right)e^{-y\sqrt{-HPr}}\,erfc\left(\frac{y}{2\sqrt{t/Pr}}-\sqrt{-Ht}\right)+\left(t+\frac{y}{2\sqrt{-H/Pr}}\right)e^{y\sqrt{-HPr}}\,erfc\left(\frac{y}{2\sqrt{t/Pr}}+\sqrt{-Ht}\right)\right] \quad (47)$$

$$f_{16}(y,t)=\frac{e^{a_{16}t}}{2}\left[e^{-y\sqrt{\Pr(a_{16}-H)}}\,erfc\left(\frac{y}{2\sqrt{t/Pr}}-\sqrt{(a_{16}-H)t}\right)+e^{y\sqrt{\Pr(a_{16}-H)}}\,erfc\left(\frac{y}{2\sqrt{t/Pr}}+\sqrt{(a_{16}-H)t}\right)\right] \quad (48)$$

$$h_1(y,t)=a_{10}f_4(y,t)+a_8f_{13}(y,t)+a_9f_{14}(y,t) \quad (49)$$

$$h_2(y,t)=a_{19}f_3(y,t)+a_{17}f_{15}(y,t)+a_{18}f_{16}(y,t) \quad (50)$$

Solutions for Plate with Constant Temperature: In order to understand effects of ramped temperature of the plate on the fluid flow, we must compare our results with constant temperature. In this case, the initial and boundary conditions are the same excluding Eq. (8) that becomes $\theta = 1\ at\ y = 0, t \geq 0$.

$$\theta(y,t)=\frac{1}{2}\left[e^{-y\sqrt{-HPr}}\,erfc\left(\frac{y}{2\sqrt{t/Pr}}-\sqrt{-Ht}\right)+e^{y\sqrt{-HPr}}\,erfc\left(\frac{y}{2\sqrt{t/Pr}}+\sqrt{-Ht}\right)\right] \quad (51)$$

Similarly, Velocity profile for isothermal temperature is

$$u=f_1(y,t)+f_{21}(y,t)+f_{22}(y,t)-f_{22}(y,t-1)H(t-1)-f_{23}(y,t)+f_{24}(y,t) \quad (52)$$

Where

$$F_{17}(y,s)=\frac{a_{32}}{s-b_4}+\frac{a_{33}}{s-b_5} \quad (53)$$

$$F_{18}(y,s)=\frac{a_{34}}{s}+\frac{a_{35}}{s-b_9}+\frac{a_{36}}{s-b_{10}} \quad (54)$$

$$F_{19}(y,s)=\frac{a_{37}}{s-b_9}+\frac{a_{38}}{s-b_{10}}+\frac{a_{39}}{s-a_{16}} \quad (55)$$

$$F_{20}(y,s)=\frac{a_{40}}{s-b_4}+\frac{a_{41}}{s-b_5}+\frac{a_{42}}{s-a_{16}} \quad (56)$$

$$F_{21}(y,s)=F_5(y,s)F_{17}(y,s) \quad (57)$$

$$F_{22}(y,s)=F_6(y,s)F_{18}(y,s) \quad (58)$$

$$F_{23}(y,s)=F_6(y,s)F_{19}(y,s) \quad (59)$$

$$F_{24}(y,s)=F_5(y,s)F_{20}(y,s) \quad (60)$$

Inverse Laplace transform of equation (53) to (60) are

$$f_{17}(y,t)=a_{32}e^{b_4t}+a_{33}e^{b_5t} \quad (61)$$

$$f_{18}(y,t)=a_{34}+a_{35}e^{b_9t}+a_{36}e^{b_{10}t} \quad (62)$$

$$f_{19}(y,t)=a_{37}e^{b_9t}+a_{38}e^{b_{10}t}+a_{39}e^{a_{16}t} \quad (63)$$

$$f_{20}(y,t)=a_{40}e^{b_4t}+a_{41}e^{b_5t}+a_{42}e^{a_{16}t} \quad (64)$$

$$f_{21}(y,t)=f_5(y,t)*f_{13}(y,t) \quad (65)$$

$$f_{22}(y,t)=f_6(y,t)*f_{14}(y,t) \quad (66)$$

$$f_{23}(y,t)=f_6(y,t)*f_{15}(y,t) \quad (67)$$

$$f_{24}(y,t)=f_5(y,t)*f_{16}(y,t) \quad (68)$$

From velocity, temperature and concentration fields, the expressions for Nusselt number, skin friction and Sherwood number can easily be determined. They are measures of the heat transfer rate and shear stress at the boundary.

Nusselt Number:

The Nusselt number Nu can be written as

$$N_u=-\left(\frac{\partial\theta}{\partial y}\right)_{y=0} \quad (69)$$

Using the equation (30), we obtained the Nusselt number for Ramped wall temperature

$$N_u=-[J_{15}(t)-J_{15}(t-1)H(t-1)] \quad (70)$$

Using the equation (42), we obtained the Nusselt number for isothermal temperature

$$Nu=-J_3(t) \quad (71)$$

Sherwood Number:

Sherwood Number is defined and denoted by the formula

$$s_h=-\left(\frac{\partial C}{\partial y}\right)_{y=0} \quad (72)$$

Using the equation (31), we obtained the Sherwood Number for Ramped wall temperature

$$s_h=-[J_{25}(t)-J_{25}(t-1)H(t-1)+J_{26}(t)-J_{26}(t-1)H(t-1)] \quad (73)$$

Skin Friction:

Skin friction, in dimensionless form, is

$$\tau_w(t) = \tau(y,t)\ at\ y = 0 \tag{74}$$

Where the shear stresses $\tau(y,t)$

$$\tau(y,t) = \left(1 + \alpha \frac{\partial}{\partial t}\right)\frac{\partial u}{\partial y} \tag{75}$$

Using the equation (32) we find the shear stress for ramped temperature as

$$\tau(y,t) = J_1(t) + J_{10}(t) - J_{10}(t-1)H(t-1) + J_{11}(t) - J_{11}(t-1)H(t-1) + J_{12}(t) - J_{12}(t-1)H(t-1) \tag{76}$$

Where

$$J_i(t) = \left.\frac{df_i}{dy}\right|_{y=0}, i = 1\ to\ 24 \tag{77}$$

$$J_i(t) = \left.\frac{dh_i}{dy}\right|_{y=0}, i = 25, 26 \tag{78}$$

IV. RESULT AND DISCUSSION:

To get perfect understanding for physics of the problem, we find numerical solution of velocity, temperature and concentration using Matlab software, obtained results presented graphically. Effects of several involved parameters are described in Figure 2 to Figure 10.

Fig. 2 shows effect of second grade fluid parameter α on velocity profile for both thermal condition, ramped wall temperature with ramped surface concentration and isothermal temp with ramped surface concentration. It is seen that second grade parameter tends to reduce velocity throughout region. It is also clear that, the velocity approaches to zero at the far away from the plate. For ramped temperature on the plate, fluids flow slower than for the constant plate temperature.

Fig.3 depicts the velocity profile for various values of k. It is observed that, for both thermal cases, velocity increases with increase in k. A similar behavior was also expected, because when we increase the permeability, due to decreasing effects of drag force wholes becomes large in porous medium and hence velocity increases. Fig.4 shows the effect of the magnetic field on velocity. It is seen that, for both heating cases, velocity decreases with increase in magnetic parameter M. The present phenomena occur when magnetic field can induce current in the conductive fluid and create Lorentz force on the fluid in the boundary layer, which slow down the velocity of the fluid. Therefore, the magnetic field acts like a drag force. The practice of magnetic fields has effectively been applied to monitoring melt convection in solidification systems.Fig. 5 show temperature profile for different values of Prandtl number Pr, when the other parameters are fixed. For both thermal conditions, it is observed that temperature of the fluid decreases with increasing Prandtl number Pr. Fig.6 illustrates that concentration profile is displayed with the variations in Schmidt number Sc. It is observed that concentration decreases with increase in Schmidt number Sc. We also observe that, due to enhancement in the values of *Sc*, the concentration near the plate gets reducing the thickness this leads minimizing the mass buoyancy force.The mass Grashof number Gm means ratio of buoyancy force and viscous hydrodynamic force and thermal Grashof number Gr indicates the ratio of thermal buoyancy force to viscous hydrodynamic force. It is observed that velocity rises with increase in Gm or Gr in Fig. 7-8 respectively. This implies that motion of fluid accelerated due to improvement in either temperature buoyancy force or mass buoyancy force. Physically, Increase in Gr indicates increase in the strength of the flow, small viscous effects in the momentum equation and thus, reasons the increase in velocity profiles. Fig. 9 shows that temperature profile for different values of heat generation H. It is seen that, heat generation H parameter is the important role in MHD fluid flow problem. It is observe that heat generation tends to improve temperature profile because of that when the amount of heat generated the bond holding the components of the fluid particles is easily broken and the fluid temperature will increased. Fig. 10 shows that concentration profile for different values of Soret number Sr. It is observe that as soret number increase concentration also increase.

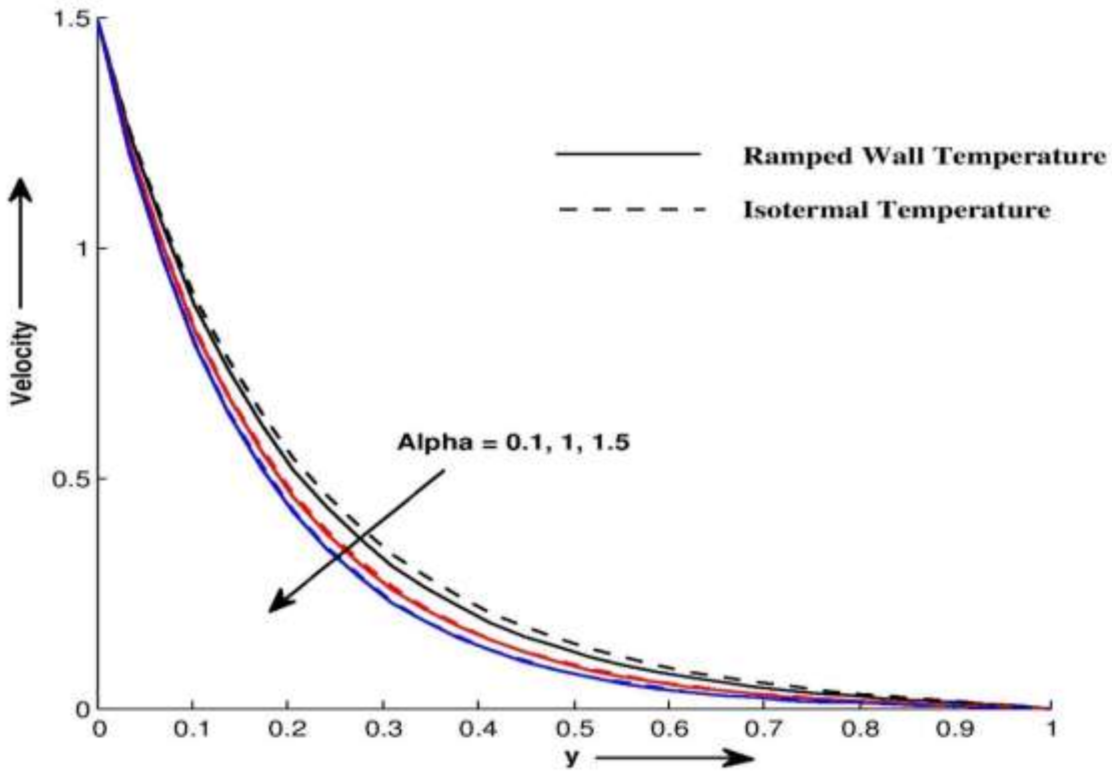

Figure 2: Velocity profile u for different values of y and α at $\mathbf{M = 5, k = 0.5, Pr = 7, Sc = 0.66, Gm = 3, Gr = 2, H = 5, Sr = 5}$ and $\mathbf{t = 0.4}$

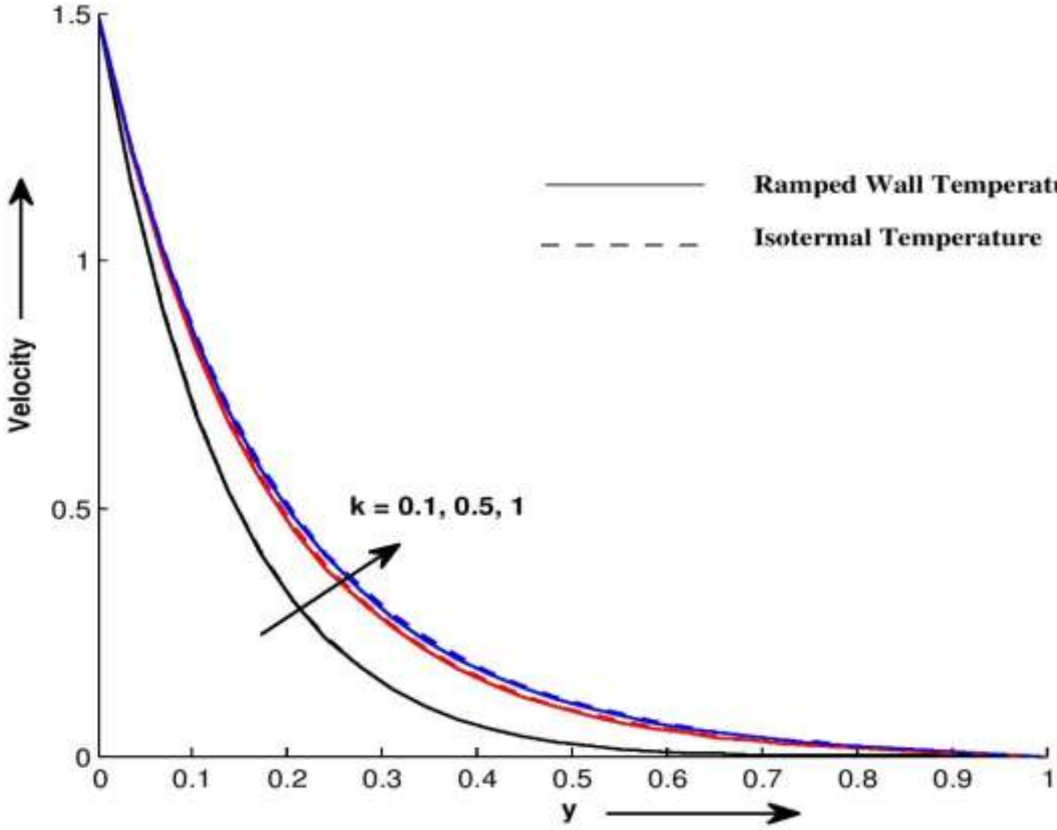

Figure 3: Velocity profile u for different values of y and k at $M = 5, \alpha = 1, Pr = 7, Sc = 0.66, Gm = 3, Gr = 2, H = 5, Sr = 5$ and $t = 0.4$

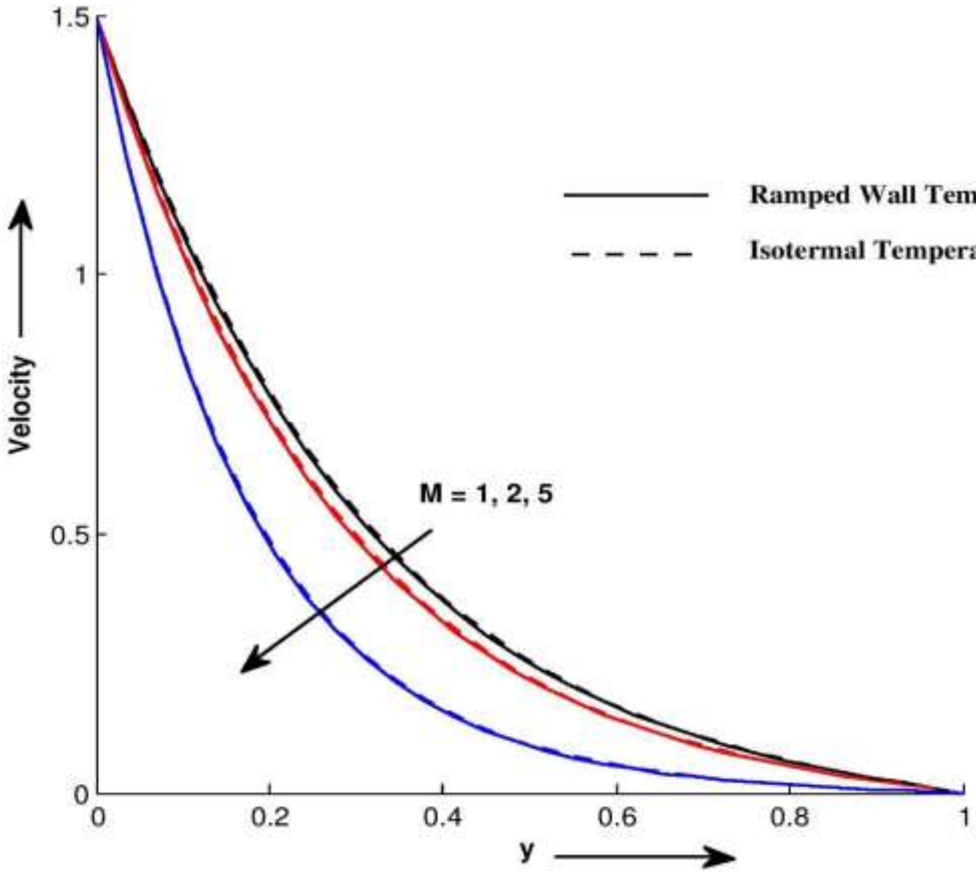

Figure 4: Velocity profile u for different values of y and M at $k = 0.5, \alpha = 1, Pr = 7, Sc = 0.66, Gm = 3, Gr = 2, H = 5, Sr = 5$ and $t = 0.4$

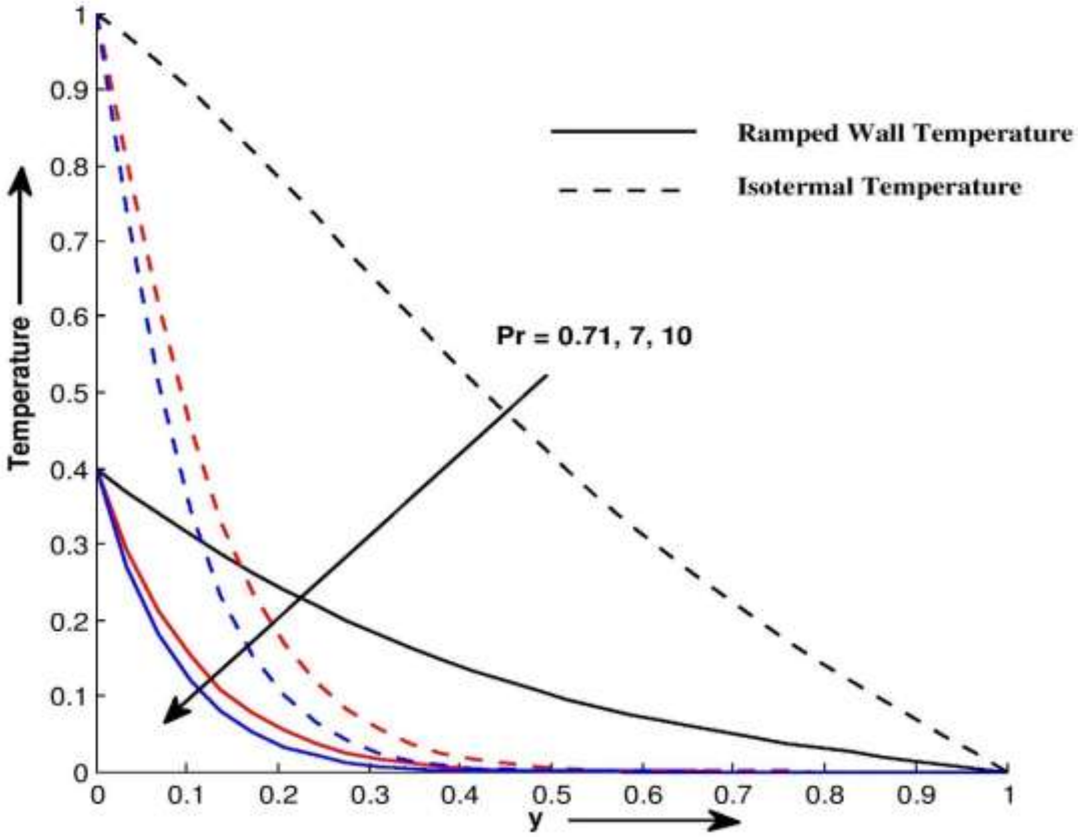

Figure 5: Temperature profile θ for different values of y and Pr at H = 5 and t = 0.4

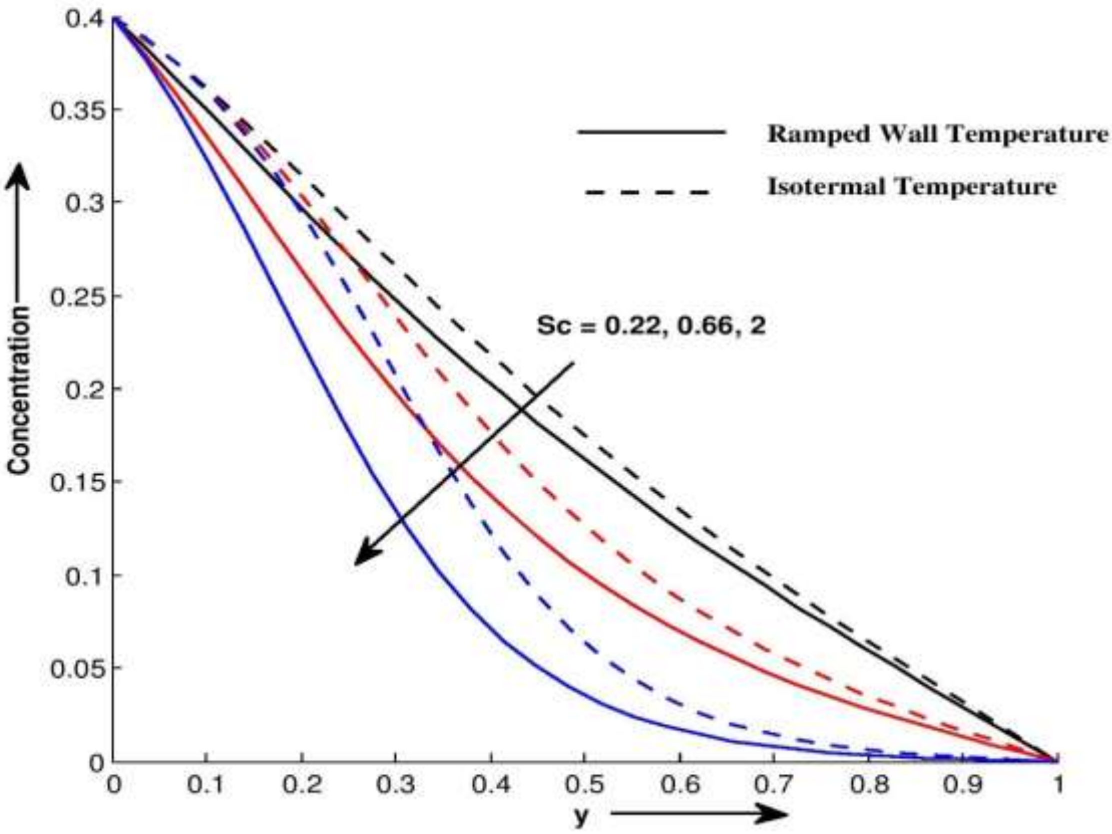

Figure 6: Concentration profile C for different values of y and Sc at Sr = 5 andt = 0.4

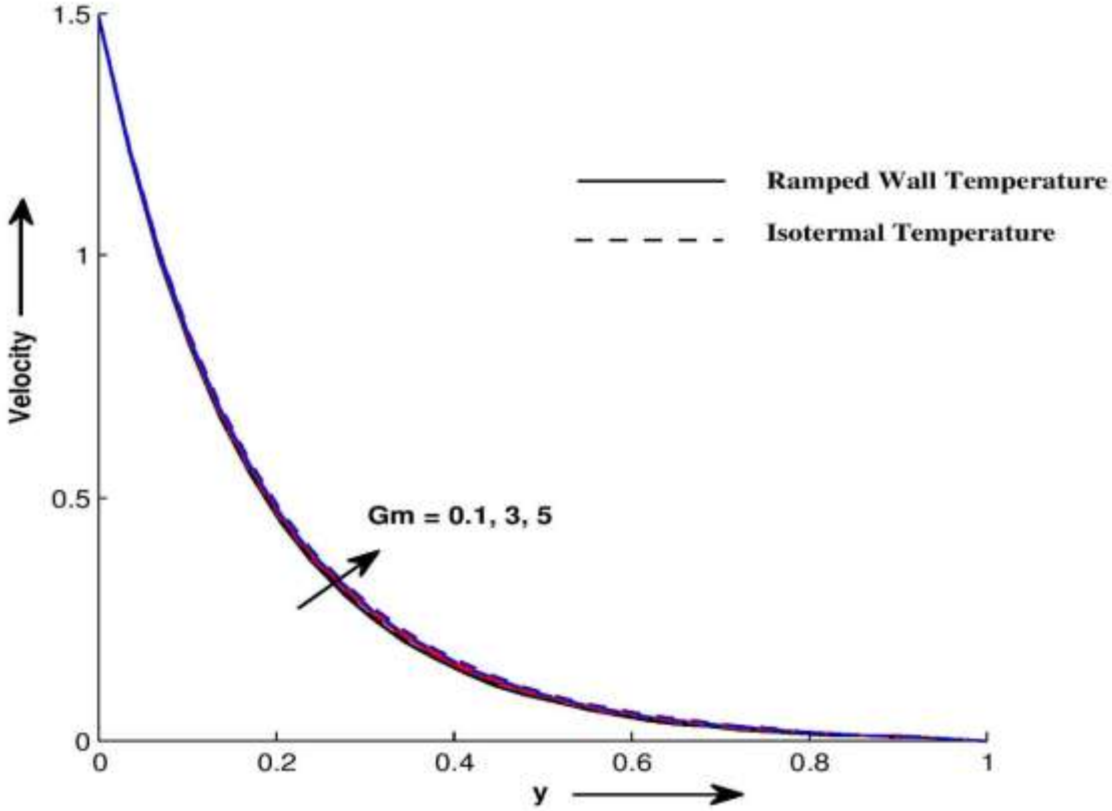

Figure 7: Velocity profile u for different values of y and Gm at $M = 5, \alpha = 1, k = 0.5, Pr = 7, Gr = 2, Sc = 0.66, H = 5, Sr = 5$ and $t = 0.4$

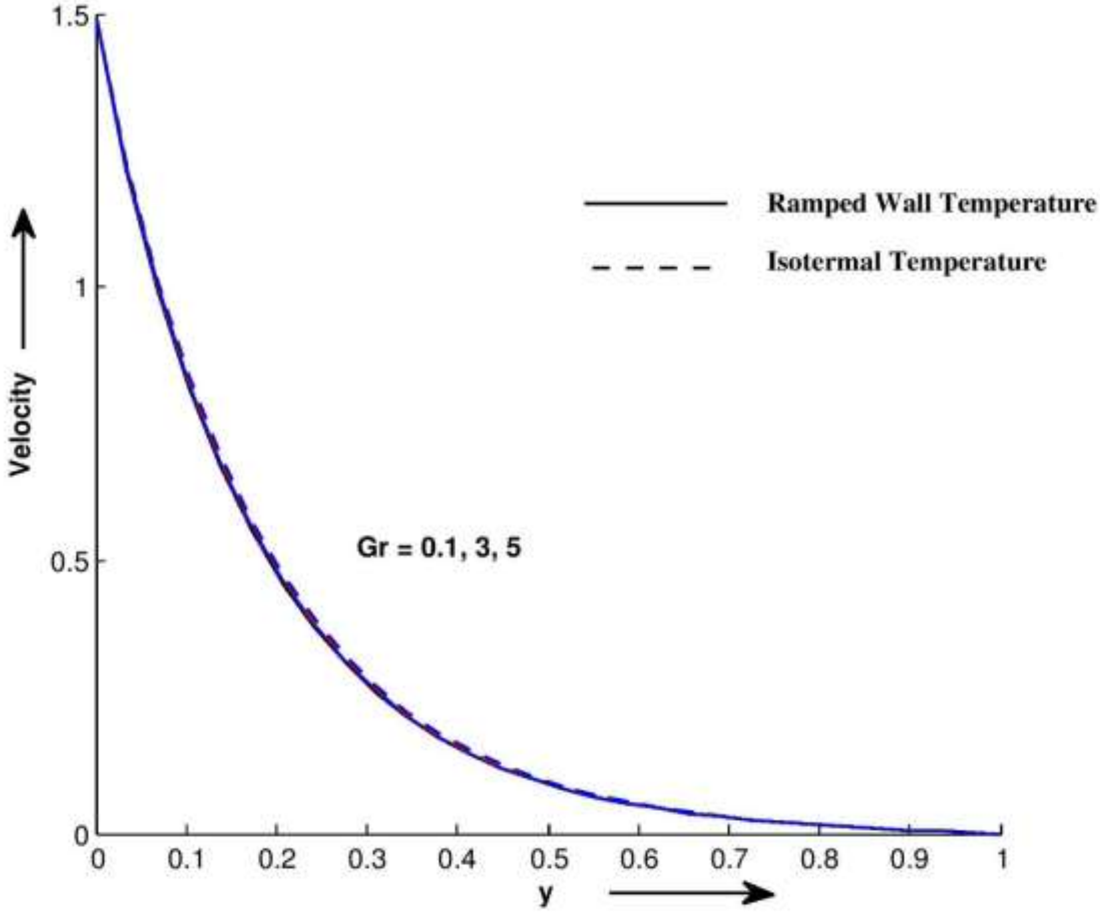

Figure 8: Velocity profile u for different values of y and Gr at $M = 5, \alpha = 1, k = 0.5, Pr = 7, Sc = 0.66, Gm = 3, H = 5, Sr = 5$ and $t = 0.4$

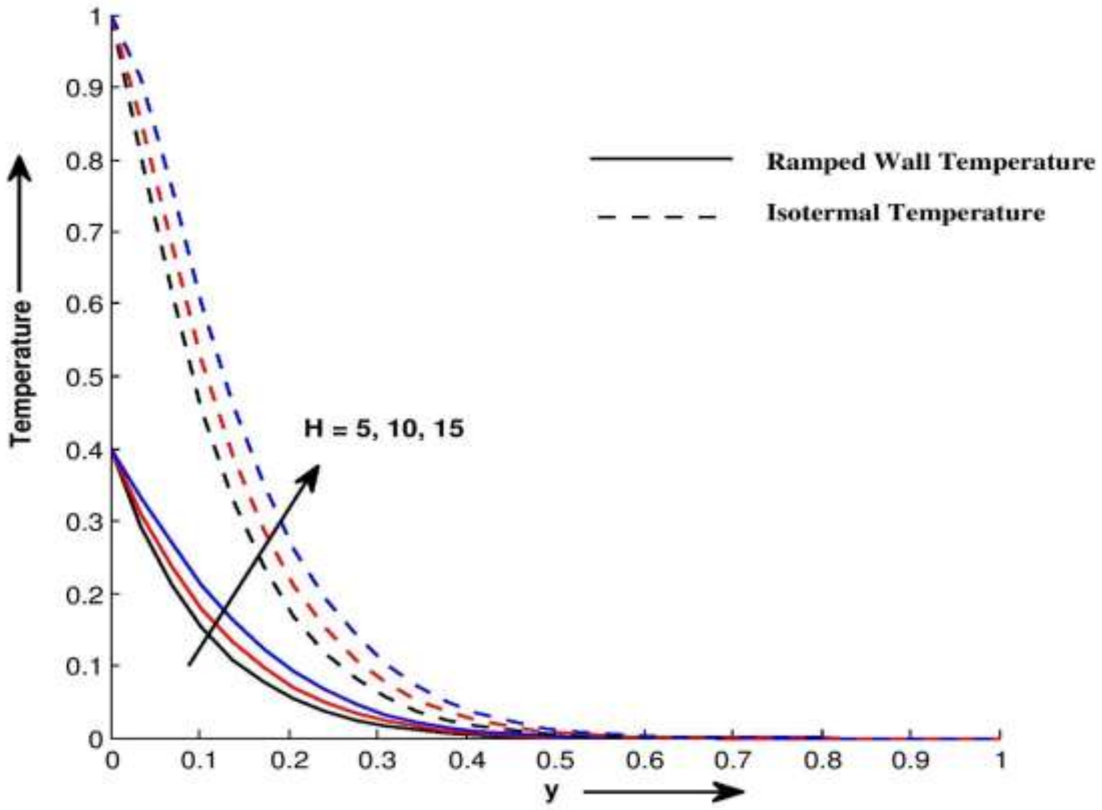

Figure 9: Temperature profile θ for different values of y and H at $\mathrm{Pr} = 7$ and $\mathrm{t} = 0.4$

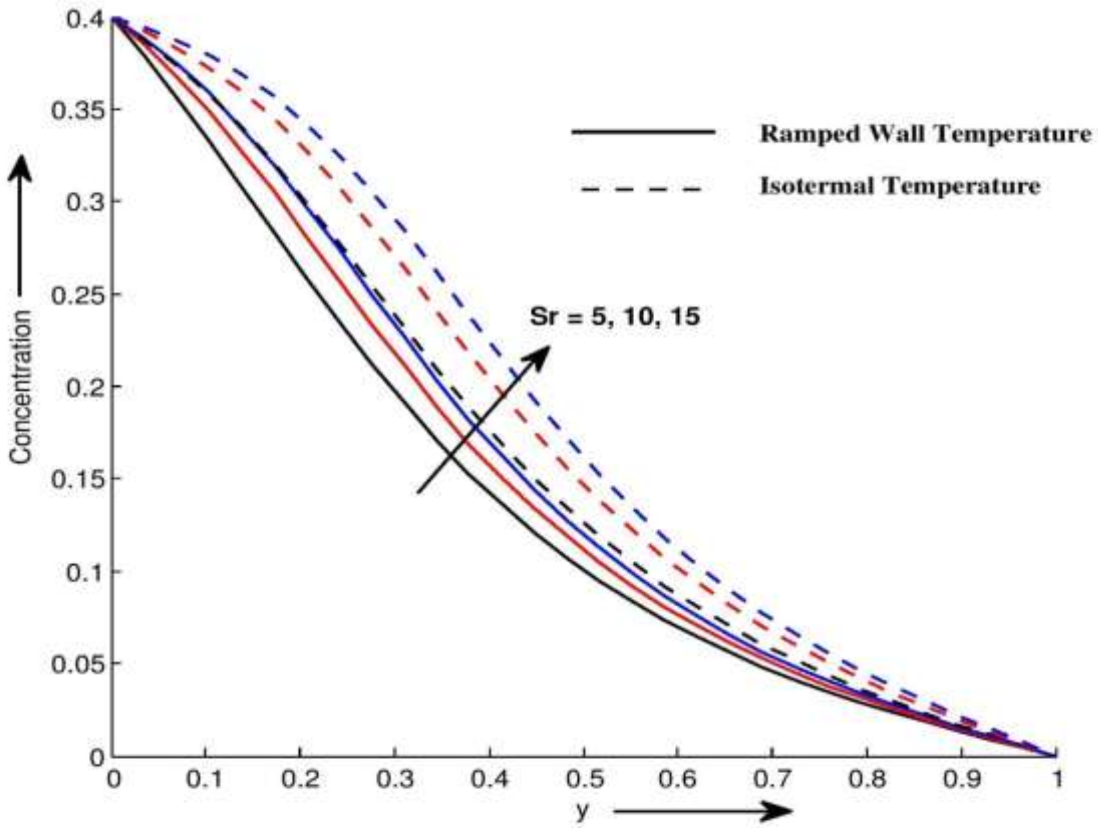

Figure 10: Concentration profile C for different values of y and Sr at $\mathrm{Sr} = 0.66$ and$\mathrm{t} = 0.4$

The numerical values of Nusselt number Nu and Sherwood number Sh, calculated from the analytical expressions are exhibited in tabular form in Tables 1 and Table 2 for both thermal cases. It is observed from Tables 1 that, for both thermal cases, Thermal radiation tends to reduced magnitude of Nusselt number whereas Prandtl number Pr have reverse effect on it. Table 2 illustrates effects of Sc and t on rate of mass transfer Sh. It is seen that, for both thermal condition, Magnitude of Sherwood number increase with increase in Schmidt number Sc. It is also seen that, for ramped wall temperature, time variable t tends to improve rate of heat and mass transfer whereas in isothermal plates time variable tends reverse effect on it.

Table 1: Nusselt number variation

Pr	T	Nusselt number for Ramped Temperature	Nusselt number for isothermal Temperature
0.71	0.4	0.6013	0.7517
7	0.4	1.8881	2.3602
15	0.4	2.7640	3.4549
7	0.5	2.1110	2.1110
7	0.6	2.3125	1.9271
7	0.7	2.4978	1.7841

Table 2: Sherwood Number variation

Sc	t	Sherwood Number Sh for Ramped Surface Concentration	Sherwood Number Sh for Constant Surface Concentration
0.22	0.4	0.3347	0.4184
0.66	0.4	0.5798	0.7247
1.0	0.4	0.7136	0.8921
0.66	0.5	0.6482	0.6482
0.66	0.6	0.7101	0.5917
0.66	0.7	0.7670	0.5478

V. CONCLUSION:

In this paper, a mathematical model is presented to investigate the thermal radiation, Heat and Mass transfer effects on Natural convective unsteady MHD second grade fluid flow with ramped wall temperature and ramped surface concentration in a porous medium. The governing dimensionless equations are solved using the Laplace transform technique. In order to determine the effect of various parameters on velocity, temperature and concentration profile, we derive the numerical solution using Matlab Software and discuss through several figures. Most important result are defined

- It is observed that velocity and temperature profile in case of ramped temperature are less than that of isothermal temperature.
- Second grade parameterα, Magnetic field M tends to de-accelerate motion of the fluid flow throughout the region, whereas permeability of porous medium k, thermal Grashof number Gr, mass Grashof number Gm tends to reverse effect on it.
- Concentration decrease with increase in Sc.
- Rate of heat transfer increase with Pr.
- Rate of mass transfer improve with Sc.

REFERENCES

[1] M. Sheikholeslami, Houman B. Rokni, Influence of EFD viscosity on nanofluid forced convection in a cavity with sinusoidal wall, Journal of Molecular Liquids,2017. http://dx.doi.org/10.1016/j.molliq.2017.02.042

[2] M. Sheikholeslami, Magnetohydrodynamic nanofluid forced convection in a porous lid driven cubic cavity using Lattice Boltzmann Method, Journal of Molecular Liquids,2017. 10.1016/j.molliq.2017.02.020

[3] M. Sheikholeslami, M. M. Bhatti, Active method for nanofluid heat transfer enhancement by means of EHD, International Journal of Heat and Mass Transfer 109 (2017) 115–122.

[4] M. Sheikholeslami, S.A. Shehzad, Thermal radiation of ferrofluid in existence of Lorentz forces considering variable viscosity, International Journal of Heat and Mass Transfer 109 (2017) 82–92.

[5] M. Sheikholeslami, T. Hayat, A. Alsaedi, Numerical simulation of nanofluid forced convection heat transfer improvement in existence of magnetic field using Lattice Boltzmann Method, International Journal of Heat and Mass Transfer, 108 (2017) 1870-1883.

[6] M. Sheikholeslami, M. Shamlooei, Fe3O4- H2O nanofluid natural convection in presence of thermal radiation, International Journal of Hydrogen Energy

[7] M. Sheikholeslami, Numerical investigation of MHD nanofluid free convective heat transfer in a porous tilted enclosure, Engineering Computations

[8] M. Sheikholeslami, T. Hayat, A. Alsaedi, Numerical simulation of nanofluid forced convection heat transfer improvement in existence of magnetic field using Lattice Boltzmann Method, International Journal of Heat and Mass Transfer.

[9] H. R. Kataria, A. Mittal, (2015): Mathematical model for velocity and temperature of gravity-driven convective optically thick nanofluid flow past an oscillating vertical plate in presence of magnetic field and radiation. Journal of Nigerian Mathematical Society, 34, 303– 317.

[10] H. R. Kataria, A. S. Mittal, (2017): Velocity, mass and temperature analysis of gravitydriven convection nanofluid flow past an oscillating vertical plate in presence of magnetic field in a porous medium, Applied Thermal Engineering, 110, 864-874.

[11] M. H. Abolbashari, N. Freidoonimehr, F. Nazari, M.M. Rashidi, Entropy Analysis for an Unsteady MHD Flow past a Stretching Permeable Surface in Nano-Fluid, Powder Technology 267 (2014) 256-267.

[12] M. M. Rashidi, M. Ali, N. Freidoonimehr, B. Rostami, M. Anwar Hossain, Mixed convective heat transfer for MHD viscoelastic fluid flow over a porous wedge with thermal radiation, Advances in Mechanical Engineering, Volume 2014 (2014) Article number 735939.

[13] M.M. Rashidi, E. Erfani, Analytical Method for Solving Steady MHD Convective and Slip Flow due to a Rotating Disk with Viscous Dissipation and Ohmic Heating, Engineering Computations 29 (6) (2012) 562–579.

[14] N. Freidoonimehr, M.M. Rashidi, S. Mahmud, Unsteady MHD free convective flow past a permeable stretching vertical surface in a nano-fluid, International Journal of Thermal Sciences 87 (2015) 136-145.

[15] M.M. Rashidi, E. Momoniat, B. Rostami, Analytic approximate solutions for MHD boundary-layer viscoelastic fluid flow over continuously moving stretching surface by homotopy analysis method with two auxiliary parameters, Journal of Applied Mathematics, Volume 2012.

[16] S. Abbasbandy, T. Hayat, A. Alsaedi, M.M. Rashidi, Numerical and Analytical Solutions for Falkner-Skan Flow of MHD Oldroyd-B fluid, International Journal of Numerical Methods for Heat and Fluid Flow 24 (2) (2014) 390-401.

[17] J Zhou, M Hatami, D Song, & D Jing, (2016). Design of microchannel heat sink with wavy channel and its time-efficient optimization with combined RSM and FVM methods. International Journal of Heat and Mass Transfer, 103, 715-724.

[18] M Hatami and H. Safari. "Effect of inside heated cylinder on the natural convection heat transfer of nanofluids in a wavy-wall enclosure." International Journal of Heat and Mass Transfer 103 (2016): 1053-1057.

[19] M Hatami, D. Song, and D. Jing. "Optimization of a circular-wavy cavity filled by nanofluid under the natural convection heat transfer condition." International Journal of Heat and Mass Transfer 98 (2016): 758-767.

[20] D Song, M Hatami, Y Wang, D Jing, & Y Yang (2016). Prediction of hydrodynamic and optical properties of TiO 2/water suspension considering particle size distribution. International Journal of Heat and Mass Transfer, 92, 864-876.

[21] M Hatami, M. C. M. Cuijpers, and M. D. Boot. "Experimental optimization of the vanes geometry for a variable geometry turbocharger (VGT) using a Design of Experiment (DoE) approach." Energy Conversion and Management 106 (2015): 1057-1070.

[22] S Ghasemi, M Hatami, A K Sarokolaie, & D D Ganji (2015). Study on blood flow containing nanoparticles through porous arteries in presence of magnetic field using analytical methods. Physica E: Low-dimensional Systems and Nanostructures, 70, 146-156.

[23] M Fakour, A Vahabzadeh, D D Ganji, & M Hatami, M. (2015). Analytical study of micropolar fluid flow and heat transfer in a channel with permeable walls. Journal of Molecular Liquids, 204, 198-204.

[24] M Hatami, D. D. Ganji, and M. Gorji-Bandpy. "Experimental and thermodynamical analyses of the diesel exhaust vortex generator heat exchanger for optimizing its operating condition." Applied Thermal Engineering 75 (2015): 580-591.

[25] M Hatami, M Sheikholeslami, M Hosseini, D D Ganji, Analytical investigation of MHD nanofluid flow in non-parallel walls, Journal of Molecular Liquids 194 (2014) 251–259.

[26] M. Sheikholeslami, D.D. Ganji, M.M. Rashidi, Magnetic field effect on unsteady nanofluid flow and heat transfer using Buongiorno model, Journal of Magnetism and Magnetic Materials, 416 (2016) 164-173 doi:10.1016/j.jmmm.2016.05.026.

[27] H. R. Kataria, H. R. Patel, (2015): Effect of magnetic field on unsteady natural convective flow of a micropolar fluid between two vertical walls. Ain Shams Engineering Journal, doi. 10.1016/j.asej.2015.08.013.

[28] H. R. Kataria, H. R. Patel, (2016): Radiation and chemical reaction effects on MHD Casson fluid flow past an oscillating vertical plate embedded in porous medium, Alexandria Engineering Journal , 55, 583-595

[29] H. R. Kataria, H. R. Patel, (2016): Soret and heat generation effects on MHD Casson fluid flow past an oscillating vertical plate embedded through porous medium, Alexandria Engineering Journal 55, 2125–2137

[30] H. R. Kataria, H. R. Patel, (2016): Effect of thermo-diffusion and parabolic motion on MHD Second grade fluid flow with ramped wall temperature and ramped surface concentration, Alexandria Engineering Journal, 10.1016/j.aej.2016.1

[31] H. R. Kataria, H. R. Patel, Heat and Mass Transfer in MHD Second Grade Fluid Flow with Ramped Wall Temperature through Porous Medium, Mathematics Today Vol.32 (2016) 67-83.

[32] S M Rassoulinejad-Mousavi, H R Seyf, S Abbasbandy, "Heat transfer through a porous saturated channel with permeable walls using two-equation energy model", Journal of Porous Media, 2013, 16 (3), 241-254.

[33] S M Rassoulinejad-Mousavi, S Abbasbandy, "Analysis of Forced Convection in a Circular Tube Filled With a Darcy–Brinkman–Forchheimer Porous Medium Using Spectral Homotopy Analysis Method". ASME. J. Fluids Eng., 2011,133(10),101207.

[34] H R Seyf, S M Rassoulinejad-Mousavi, "An Analytical Study for Fluid Flow in Porous Media Imbedded Inside a Channel With Moving or Stationary Walls Subjected to Injection/Suction", ASME. J. Fluids Eng., 2011, 133(9), 091203.

[35] S K Mohammadian, S M Rassoulinejad-Mousavi, Y Zhang, "Thermal management improvement of an air-cooled high-power lithium-ion battery by embedding metal foam", Journal of Power Sources, 2015, 296, 305-313.

[36] S M Rassoulinejad-Mousavi, S Abbasbandy, H H Alsulami, "Analytical flow study of a conducting Maxwell fluid through a porous saturated channel at various wall boundary conditions", Eur. Phys. J. Plus, 2014, 129: 181.

[37] S M Rassoulinejad-Mousavi, H Yaghoobi, "Effect of Non-linear Drag Term on Viscous Dissipation in a Fluid Saturated Porous Medium Channel with Various Boundary Conditions at Walls", Arab. J. Sci. Eng. , 2014, 39 (2), 1231–1240.

[38] R. Cortell, MHD flow and mass transfer of an electrically conducting fluid of second grade in a porous medium over a stretching sheet with chemically reactive species, Chemical Engineering and Processing: Process Intensification 46(2007),721–728

[39] T. Hayat, C. Fetecau, M. Sajid, Analytic solution for MHD Transient rotating flow of a second grade fluid in a porous space, Nonlinear Analysis: Real World Applications, 9(2008),1619–1627

[40] T. Hayat, S. Saif, Z. Abbas, The influence of heat transfer in an MHD second grade fluid film over an unsteady stretching sheet, Physics Letters A, 372(2008), 5037–5045

[41] T. Hayat, I. Naeem, M. Ayub, A.M. Siddiqui, S. Asghar, C.M. Khaliqu, Exact solutions of second grade aligned MHD fluid with prescribed vorticity, Nonlinear Analysis: Real World Applications, 10(2009),2117–2126

[42] T. Hayat,I. Ullah,T. Muhammad, A. Alsaedi, Magnetohydrodynamic (MHD) three-dimensional flow of second grade nanofluid by a convectively heated exponentially stretching surface, Journal of Molecular Liquids, 220(2016),1004–1012.

[43] A. S. Bataineh, O.R. Isik, I. Hashim, Bernstein method for the MHD flow and heat transfer of a second grade fluid in a channel with porous wall, Alexandria Engineering Journal (2016), http://dx.doi.org/10.1016/j.aej.2016.06.022 1110-0168.